Reaction Kinetics, Mechanisms and Catalysis (2023) 136:653–670
https://doi.org/10.1007/s11144-023-02365-4

Application of mixture experimental design for optimization of nickel catalyst promoted with Cu and Mg and supported by kieselguhr for soybean oil hydrogenation

Y. Shaveisi[1] · **S. Sharifnia**[1]

Received: 16 December 2022 / Accepted: 4 February 2023 / Published online: 15 February 2023
© Akadémiai Kiadó, Budapest, Hungary 2023

Abstract

In this work, Ni/calcined Kieselguhr was promoted with Cu and Mg to enhance the hydrogenation of soybean oil. The experimental design software was used to study the impact of each metal on catalyst activity and find the best Ni–Cu–Mg composition. The prepared catalysts were characterized by BET, FESEM, EDX-elemental mapping and H_2-TPR analyses. The catalytic activity of all prepared catalysts was examined in a semi-batch reactor. The best catalytic composition was obtained to be 0.604 Ni, 0.223 Cu, and 0.173 Mg values (based on the mass fraction of the prepared catalyst with the total activated catalyst weight of 21 wt%). The highest catalytic activity and fatty acid conversion, 77.6 IV and 69.0% linoleic acid conversion, were found at optimum conditions. Kinetic studies indicated that the reaction rate depends on catalyst composition. The optimum catalyst exhibited a significant rate constant for linolenic and linoleic acid conversion with the selectivity of 1.212 and 2.218.

Keywords Soybean oil hydrogenation · Nickel catalyst · Promoted catalyst · Experimental design

✉ S. Sharifnia
sharif@razi.ac.ir

Y. Shaveisi
yasershavisi@gmail.com

[1] Chemical Engineering Department, Catalyst Research Center, Razi University, Kermanshah 67149-67246, Iran

Introduction

Hydrogenation of oil converts unsaturated acids into saturated ones and improves its shelf life. It is possible to manipulate the fatty acid composition and achieve the desired properties using partial hydrogenation of oil. Nickel, copper, platinum, and palladium are the most common metals being used as active species in heterogeneous catalysts for partial hydrogenation of polyunsaturated triglycerides [1, 2]. Although noble metal catalysts such as platinum or palladium are highly active, they are too costly and yield products of less desirable characteristics [3]. Owing to the availability, low cost, and inert nature of Nickel relative to oil, hydrogenation with nickel catalysts has been the suitable choice of industry. Nickel interacts with oil components and forms salts dissolvable in oil [4–6].

The typical nickel catalyst system for the hydrogenation of edible oil is composed of ca. 22 wt% reduced Nickel deposited on a suitable support and dispersed into oil in the absence of air [7]. Support type and the chemical preparation, the technique of Nickel and promoter deposition, particle size, pore size and pore size distribution of the support, and the activation procedure are all critical factors affecting the activity and selectivity of the catalyst [8, 9]. Kieselguhr [10], bentonite [11], activated carbon [12], perlite [13], alumina [14, 15], waterglass [4], and zeolites [16, 17] have been used as catalyst support for the hydrogenation of edible oils. Industrial oil hydrogenation is commonly performed with a nickel catalyst supported on Kieselguhr, a mineral mainly containing amorphous SiO_2 with excellent chemical, thermal, and textural properties [18].

Kieselguhr, diatomaceous earth, is a siliceous (mainly silicon oxide) sedimentary rock consisting principally of the fossilized skeletal remains of a diatom, a unicellular aquatic plant. Due to it is a cheaper price, porous structure, low density, and chemical inertness, It's widely utilized as a filter aid, carrier material for lipase, immobilization, and stable catalyst support.

Hydrogenation process by Nickel catalysts is carried out at high temperatures (≥ 180 °C), which increases the formation of trans-isomers and by-products from the thermal decomposition of fatty acids. Nickel catalysts can be promoted with metals and metal oxides to solve its limitations, such as high reaction temperature and deactivation due to poisoning [19]. The base metals, such as copper and magnesium, can be used as promoters of Nickel to extend the lifetime of the host catalyst and maintain the catalytic activity at a high level [20].

The present study aims at modeling the content of fatty acids in soybean oil as a function of catalyst composition. The Simplex Lattice Mixture Design (SLMD) was used to evaluate the effect of Cu and Mg promoters on the catalytic activity and selectivity of Ni/calcined Kieselguhr particles. Kieselguhr applies as a support in the preparation of catalyst samples. The prepared catalysts were studied by BET, FESEM, EDX-elemental mapping and H_2-TPR analyses. The hydrogenation process was carried out in a semi-batch reactor. The kinetics and selectivity of catalytic reactions were discussed in detail.

Table 1 Composition of soybean oil

Component	Value
Linolenic acid ($C_{18,3}$)	6.58
Linoleic acid ($C_{18,2}$)	51.35
Oleic acid ($C_{18,1}$)	25.22
Stearic acid ($C_{18,0}$)	4.01
IV	127

Table 2 Chemical composition and physical properties of calcined Kieselguhr and optimum metlats/calcined Kieselghur catalyst

Compound	Calcined kieselguhr	Optimum catalyst
pH (1:3 water)	9	8
Particle size (μm)	≥ 1	≤ 37
SiO_2 (%)	≥ 91.8	71.08
Al_2O_3 (%)	≤ 4.2	3.32
Fe_2O_3 (%)	≤ 1.28	1.07
P_2O_3 (%)	≤ 0.12	0.092
NiO	–	11.9
CuO	–	4.58
TiO_2 (%)	≤ 0.5	0.41
CaO (%)	≤ 0.42	0.34
MgO (%)	≤ 0.43	3.96
$Na_2O + K_2O$ (%)	≤ 2.2	1.69
Loss on ignition (%)	≤ 2	≤ 1

Experimental and analysis method

Materials

Soybean oil (refined) was purchased from Nazgol Co., Kermanshah, Iran. Table 1 displays the composition of the soybean oil used in this research. All chemicals used for the synthesis of catalysts were of high purity grade and purchased from Merck Co. $Ni(NO_3)_2{\cdot}6H_2O$, $Mg(NO_3)_2{\cdot}6H_2O$, and $Cu(NO_3)_2{\cdot}6H_2O$ were used as catalyst precursors. Sodium carbonate (Na_2CO_3) and sodium hydroxide (NaOH) were applied as catalyst precipitants and were purchased from Merck Co. All chemicals were applied in high purity (> 99%). Kieselguhr powder, which was employed as catalyst support, was purchased from Tabriz mineral Co and calcined in 550 °C. The chemical composition and physical properties of Kieselguhr powder are shown in Table 2.

Catalyst preparation and reduction

Aqueous solution of nickel nitrate hexahydrate ($Ni(NO_3)_2{\cdot}6H_2O$), copper nitrate hexahydrate ($Cu(NO_3)_2{\cdot}6H_2O$), and magnesium nitrate hexahydrate ($Mg(NO_3)_2{\cdot}6H_2O$)

were prepared with a desired mass ratio and heated up to 50 °C. Afterward, a desired amount of Kieselguhr support was added under stirring for 30 min (the amount of support is 79 wt% based on the weight of the reduced catalyst). Then, 2 M solution consisting of an equimolar ratio of sodium carbonate and sodium hydroxide was prepared and poured into the starting solution until pH of the precipitated suspension reached 8. The suspension was heated to.

95 °C and stirred for 60 min. The mixture was then filtered and thoroughly rinsed using deionized water three times. The final product was dried at 65 °C for 5 h in an oven and calcined at 550 °C for 2 h. All calcined samples were sieved with mesh number 400.

The activation of the prepared catalysts was performed by dry reduction method at a constant temperature of 475 °C for 2 h in a laboratory setup. The reduction process was accomplished by a gas mixture of H_2/N_2 (1:1, v/v) at a flow rate of 35 mL/min. After cooling down to room temperature, the reduced precursors were impregnated with fully hydrogenated palm oil.

Catalyst characterization

The morphology of the catalysts was determined using scanning electron microscopy.

(FE-SEM, Fei Quanta 400F) operated at 20 kV. The energy dispersive X-ray spectroscopy (EDX) was performed using an Oxford Instruments to obtain the elemental information of the catalysts.

The nitrogen adsorption–desorption isotherms are determined to the specific.

surface area, the total pore volume ($\boldsymbol{V_p}$) at $p/p^o = 0.998$ and the mean pore diameter are estimated with Win ADP (CE Instruments) using the BET method. The pore size distribution was determined using desorption isotherm and Barret–Joyner–Halenda (BJH) method in a Micromeritis TriStar II porosity analyzer. Temperature programmed reduction (TPR) was carried out with the Micromeritics AutoChem II 2920 chemisorption analyzer fitted with a thermal conductivity detector.

Hydrogenation reactor

All hydrogenation experiments were carried out in semi-batch conditions. The reactor was filled with 900 mL soybean oil and 500 mg of reduced catalyst. The hydrogenation reactor containing soybean oil and catalyst was warmed up to 120 °C in the presence of nitrogen or argon gas at atmospheric pressure to exit water and oxygen remaining inside the reactor. Then, the H_2 was flowing inside the reactor, and the H_2 flow rate was adjusted by mass flow control. The system was purged from the air with N_2 and heated and pressurized at the required conditions, maintaining a mechanical stirring rate at 750 rpm. The reactor was filled with hydrogen at 3 bar pressure and maintained under isothermal conditions (180 °C) during the hydrogenation test. The operating conditions were obtained by repeating the experiments and increasing the temperature from 120 to 180 °C heat rating was 30 °C/min. After purging residues, the oil samples were

collected from the sampling valve, and the fatty acids were analyzed with GC. The schematic of the setup is shown in Fig. S1.

GC analysis and kinetic equations

Gas chromatography analysis was applied to determine the fatty acid composition in raw and hydrogenated oils. According to State Standard (GOST), the triglycerides of fatty acids are converted into their methyl ethers, and the obtained fatty acid methyl ethers can be analyzed in a Chromos GC-1000 gas chromatograph equipped with a flame ionization detector using a capillary column with parameters 100 m×0.25 mm×0.20 μm (Agilent Technologies). Based on GC data, the iodine value (*IV*) could be calculated from the fatty acid levels via Eq. 1 [21].

$$IV = 0.95 \times C_{(16:1)} + 0.89 \times C_{(18:1)} + 1.732 \times C_{(18:2)} + 2.616 \times C_{(18:3)} + 0.785 \times C_{(20:1)}, \quad (1)$$

Here $\boldsymbol{C_{(x:y)}}$ corresponds to the sum of relative percentage concentrations of an unsaturated fatty acid with x total carbon number and y double bonds. The $\boldsymbol{IV}$ is the weight in grams of iodine absorbed by 100 g of an oil or fat. Experimentally, this can be obtained by using the Wijs' method [22].

Evaluation of the catalyst selectivity by first approximation indicates a reaction mechanism composed of a series of straight reduction steps (Eq. 2).

$$Linolenic\,(C_{18:3}) \xrightarrow{k_3} Linoleic\,(C_{18:2}) \xrightarrow{k_2} Oleic\,(C_{18:1}) \xrightarrow{k_1} Stearic\,(C_{18:0}), \quad (2)$$

Here $\boldsymbol{k_1}$, $\boldsymbol{k_2}$, and $\boldsymbol{k_3}$ are the rate constants. The concentration of all components can be expressed as a function of time (t), as shown in Eqs. 3–9.

$$\frac{dC_{(18:3)}}{dt} = -k_3 C_{(18:3)}, \quad (3)$$

$$\frac{dC_{(18:2)}}{dt} = -k_2 C_{(18:2)} + k_3 C_{(18:3)}, \quad (4)$$

$$\frac{dC_{(18:1)}}{dt} = -k_1 C_{(18:1)} + k_2 C_{(18:2)}, \quad (5)$$

$$\frac{dC_{(18:0)}}{dt} = k_1 C_{(18:0)}, \quad (6)$$

$$C_{(18:3)} = C_{(18:3:0)} \exp(-k_3 t), \quad (7)$$

$$C_{(18:2)} = \left(C_{(18:2:0)} + C_{(18:3:0)} \frac{k_3}{k_3 - k_2} \right) \exp(-k_2 t) + \left(C_{(18:3:0)} \frac{k_3}{k_2 - k_3} \right) \exp(-k_3 t), \quad (8)$$

$$C_{(18:1)} = \left(C_{(18:1:0)} + C_{(18:2:0)} \frac{k_2}{k_2 - k_1} + C_{(18:3:0)} \frac{k_2 k_3}{(k_2 - k_1)(k_3 - k_1)} \right) \exp(-k_1 t) + \frac{k_2}{k_1 - k_2} \left(C_{(18:2:0)} + C_{(18:3:0)} \frac{k_3}{k_3 - k_2} \right) \exp(-k_2 t) + \left(C_{(18:3:0)} \frac{k_2 k_3}{(k_1 - k_3)(k_2 - k_3)} \right) \exp(-k_3 t), \tag{9}$$

$$S_{Ln} = \frac{k_3}{k_2}, \tag{10}$$

$$S_{Le} = \frac{k_2}{k_1}. \tag{11}$$

According to the literature [23], the selectivity towards linolenic acid $\boldsymbol{C_{(18:3)}}$ is denoted by $\boldsymbol{S}_{\mathrm{Ln,}}$ which represents the relation $\boldsymbol{(k_3/k_2)}$ in Eq. 10, while the selectivity towards linoleic acid $\boldsymbol{C_{(18:2)}}$ is denoted by $\boldsymbol{S}_{\mathrm{Le}}$ defined by $\boldsymbol{(k_2/k_1)}$ in Eq. 11. The rate constant of the studied catalysts was determined by solving kinetic differential equations using MATLAB software.

Experimental design

Mixed-component design of experiments (MDOE) is a powerful analytical tool for analyzing the issue of multi-component mixtures, in which relative proportions of the ingredients are considered as factors affecting their response to the mixing process. Contrary to designs for independent variables, in this type of design, the proportions of constituents do not change independently, i.e., the proportion of one constituent in a $\boldsymbol{q}$-constituents mixture varies according to other $\boldsymbol{(q\text{-}1)}$ constituents as indicated by Eq. 12 [24].

$$0 \le x_i \le 1 \quad (or\ 100\%), \qquad \sum_{i=1}^{q} x_i = 1 \quad (or\ 100\%) \tag{12}$$

Here $\boldsymbol{x_i}$ is the proportion of $\boldsymbol{i^{th}}$ constituent and $\boldsymbol{q}$ is the number of constituents in the mixture. Due to this limitation, the polynomial regression presented in these designs is different from conventional equations in designs for independent variables, and there is no trace of the constant. The general form of the particular cubic regression equation, as a member of widely used mixture models, was applied in this study (Eq. 13) [25].

$$Y = \sum_{1 \le i \le q} \beta_i x_i + \sum_{1 \le i \le j \le q} \beta_{ij} x_i x_j + \sum_{1 \le i \le j \le k \le q} \beta_{ijk} x_i x_j x_k \tag{13}$$

Here $\boldsymbol{Y}$ is the dependent variable, $\boldsymbol{\beta_i}$ is the coefficient of the linear terms, $\boldsymbol{\beta_{ij}}$ is the coefficient of the two-term interactions, and $\boldsymbol{\beta_{ijk}}$ is the coefficient of the three-term

interactions. In this study, the effect of Ni (x_1), Cu (x_2), and Mg (x_3) contents on the responses, ***IV*** (iodine value), and linolenic acid conversion (%), was investigated. The Design-Expert 12 software (Stat-Ease Inc., Minneapolis, USA) was applied for planning the experiments. 10 runs were designed, including 3 pure-constituent blends (vertices of the triangle), 3 two-constituent blends (arranged at the edges of the triangle), and 4 three-constituent blends (inside of the triangle), as illustrated in Fig. S2. The vertices point was replicated to confirm the reproducibility of the process. Therefore, the total number of experiments was 11 runs. The experimental design matrix and the variables and their levels are presented in Table 3. It should be noted that the calculations are based on the mass fraction of metal component, and the total weight percent of Ni–Cu–Mg catalyst is 21 wt%.

Results and discussions

Catalyst characterizations

N_2 adsorption–desorption measurements were applied to investigate the physico-chemical properties of the calcined Kieselghur, metals catalyst, and metals/calcined Kieselghur catalyst and listed in Table 4. From Table 4, Kieselghur has a higher specific surface area and pore volume than other prepared samples. The pores of the catalyst must be large enough so that the active metal is accessible to triglyceride molecules. It can also be observed that the unsupported Ni catalyst has a higher specific surface area than the Ni/Kieselghur catalyst. The decrease in the surface area Ni/Kieselghur catalyst can be related to the partial blockage of the Kieselghur pores. On the other hand, adding metals such as Cu and Mg decreases the specific surface area in the Ni catalyst with and without Keiselghur support.

The obtained BET graphs for (Ni–Cu–Mg)/Kieselghur catalyst are shown in Fig. 1. Obviously, the catalyst shows type II isotherm with a small H3 hysteresis

Table 3 Mass fractions Ni, Cu and Mg generated by the simplex lattice mixture design (based on 21 wt% of reduced catalyst)

Coded component	Constituent mass fractions		
	Ni (x_1)	Cu (x_2)	Mg (x_3)
A	1	0	0
B	0.75	0.25	0
C	0.5	0.5	0
D	0.833	0.083	0.083
E	1	0	0
F	0.5	0	0.5
G	0.75	0	0.25
H	0.667	0.167	0.167
I	0.583	0.333	0.083
J	0.5	0.25	0.25
K	0.583	0.083	0.333

Table 4 BET surface area and pore size of the calcined Keiselghur, metals catalyst and metals on the calcined Kiesleghur catalyst

Support and catalyst	Metal loading (wt%)	BET area (m^2/g)	Total volume (mm^3/g)	Mean pore diameter (nm)
Calcined Kieselghur	–	16.38	56.17	7.28
Ni	Ni (100)	9.3	15.94	17.50
Ni–Cu–Mg	Ni(60.38),Cu(22.35),Mg(17.27)	3.9	12.70	19.76
Ni/Kieselghur	Ni (21)	8.41	21.63	8.34
Ni–Cu–Mg/Kieselghur	$^{++}$Ni(60.38),Cu(22.35) ,Mg(17.27)	5.064	38.99	7.99

$^{++}$All metal composition is 21wt% of supported catalyst (79wt% Kieselguhr)

loop, confirming the macroporous feature of the catalyst. This isotherm shape is reported in the literature as pseudo-type II [26]. Based on the BET and BJH methods, the catalyst exhibited surface area, average pore size, and pore volume of 5.064 m^2/g, 7.99 nm, and 38.99 mm^3/g. Such a low surface area is in agreement with the macroporosity feature.

Fig. 2 depicts the FESEM images of the calcined Kieselghur and the calcined catalyst (Ni–Cu–Mg/calcined Kieselghur). From Fig. 2a, the surface of the Kieselghur is uniform and consists of fragments with different shape and pore size. This rough surface with holes is suitable for the support of the catalyst particles. It can be seen from Fig. 2b that the surface of the calcined Kieselghur was covered with numerous fine metals catalyst particles with an effective diameter between 22 and

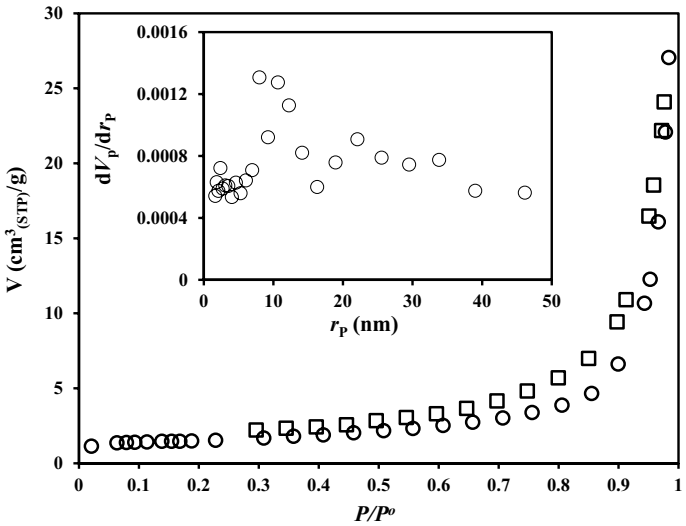

Fig. 1 N_2 adsorption–desorption isotherm, and BJH pore size distribution of the calcined Kieselghur

44 nm (Fig. S3). From the mapping and EDX analyses illustrated in Fig. 3, all the constituent elements of the (Ni–Cu–Mg)/calcined Kieslghur were detected in a uniform distribution.

To investigate the redox properties of the Ni/calcined Kieselghur before and after promoting with Cu and Mg, H_2-TPR was used, and the results are shown in Fig. 4. The reduction profile of the Ni/calcined Kieselghur are characterized by two reduction peaks at 585 and 715 °C which were shifted to 472 and 545 °C after promoting Ni by Cu and Mg, respectively. Shifting the peaks towards low temperature in the Ni–Cu–Mg on the calcined Kieselghur is attributed to the presence of copper and magnesium metals which were confirmed by EDX analysis.

The required high temperature for nickel catalysts indicates the existence of difficult reducible compounds. It has been reported that nickel hydroxide reacts with the silica and alumina supports and forms nickel hydrosilicate and hydroaluminate,

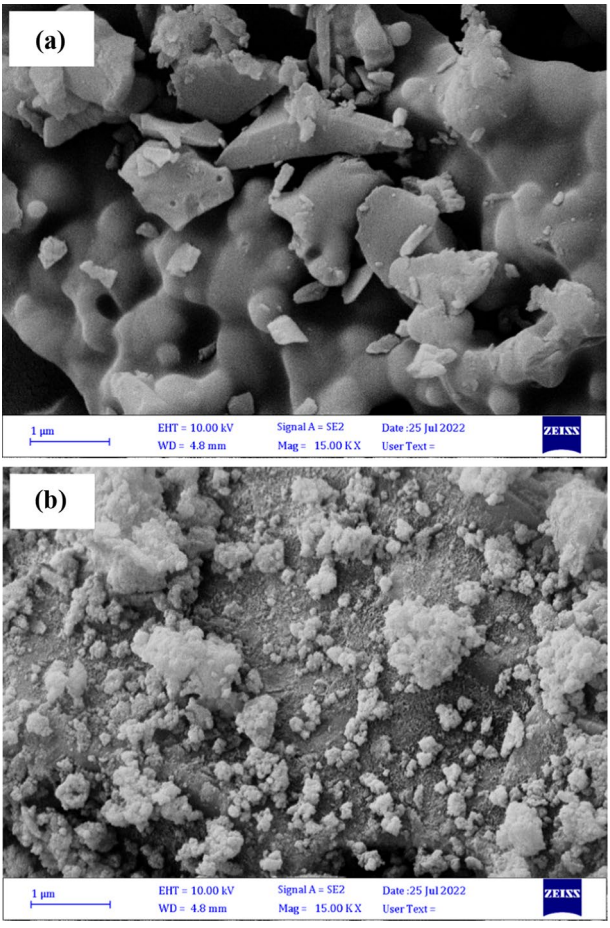

Fig. 2 FESEM images of **a** calcined Kieselguhr, and **b** Ni–Cu–Mg particles on the calcined Kieselguhr

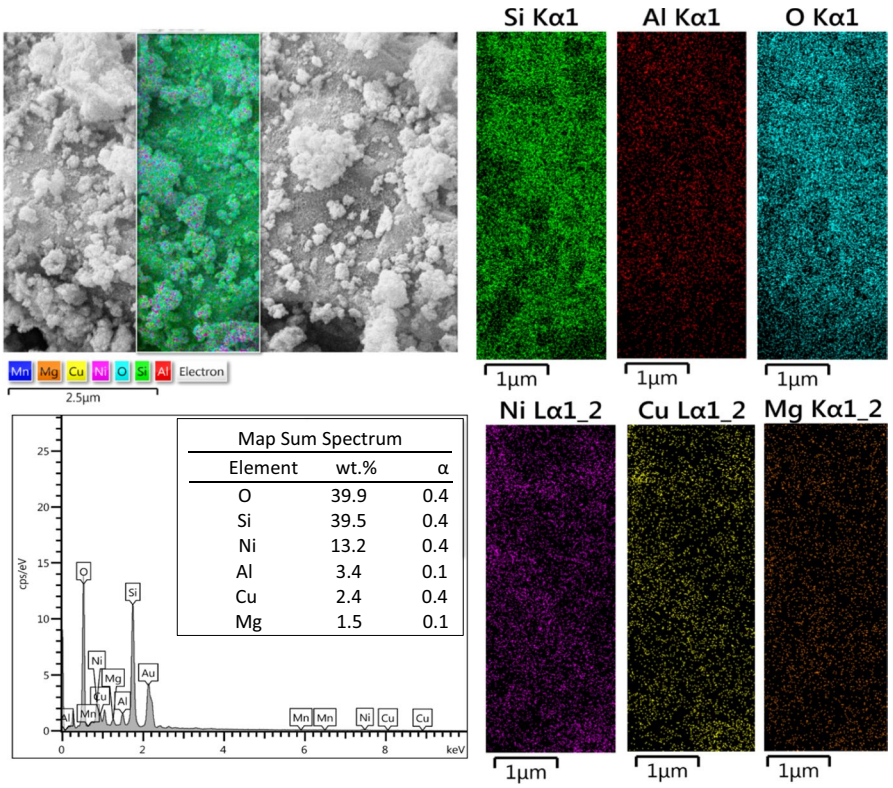

Fig. 3 Elemental mapping and EDX spectra of (Ni–Cu–Mg)/calcined Kieselguhr catalyst

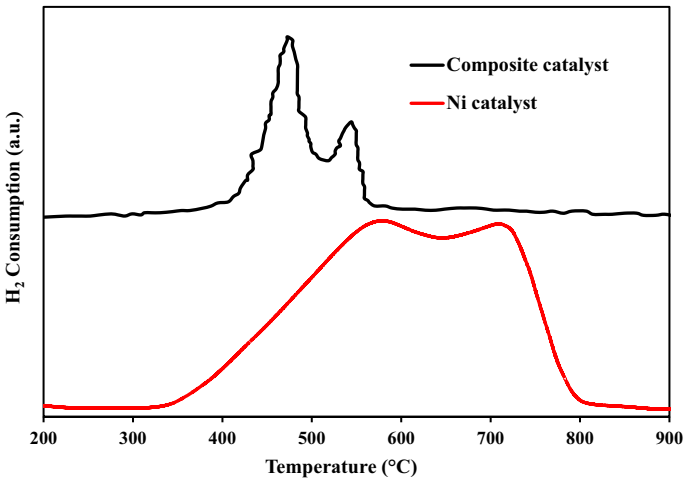

Fig. 4 Temperature programed reduction (TPR) of Ni/calcined Kieselguhr and (Ni–Cu–Mg)/ calcined Kieselguhr catalysts

highly dispersed phases. For the nickel hydroaluminate form, the reduction peak occurs at a slightly lower temperature. Also, when Ni is doped with Cu, Cu^{2+} can be reduced at lower temperatures because it has a higher standard reduction potential ($Cu^{2+}/Cu^0 + 0.34$ V) than Ni^{2+} ($Ni^{2+}/Ni^0 - 0.26$ V). It has been observed that metallic copper increases the reducibility of Ni species because metallic copper can dissociate the hydrogen molecule into hydrogen atoms, which can drop to the neighboring NiO surface. This resulted in a lower temperature reduction in NiO–CuO metal oxides compared to NiO. For the Mg effect, H_2 consumption occurs over a wider temperature window and peaks at a relatively high temperature. Therefore, Mg is presented as an oxide in the reduced sample catalysts.

Evaluation of soybean oil hydrogenation by the reduced catalyst

Two responses were considered for soybean oil hydrogenation, iodine value ($\boldsymbol{Y_1}$) and linoleic acid conversion ($\boldsymbol{Y_2}$). The design expert software proposed cubic polynomial models for the prediction of $\boldsymbol{Y_1}$ and $\boldsymbol{Y_2}$ as function of input variables (Eqs. 12 and 13). The experimental and predicted values of the responses are shown in Table 5.

$$Y_1 = 94.14x_1 + 86.62x_2 + 89.53x_3 - 25.94x_1x_2 - 16.12x_1x_3 - 31.69x_2x_3 - 259.70x_1x_2x_3, \tag{14}$$

$$Y_2 = 35.16x_1 + 51.14x_2 + 45.48x_3 + 55.73x_1x_2 + 34.73x_1x_3 + 64.75x_2x_3 + 169.78x_1x_2x_3. \tag{15}$$

The significance of each term in the models was evaluated by *P*-value; the results are shown in Table 6. Considering *P*-value < 0.05, all input variables of $\boldsymbol{x_1}$, $\boldsymbol{x_2}$, and $\boldsymbol{x_3}$, the mutual interactions of $\boldsymbol{x_1x_2}$, $\boldsymbol{x_1x_3}$, and $\boldsymbol{x_2x_3}$, and the triple interaction of $\boldsymbol{x_1x_2x_3}$ are significant for both $\boldsymbol{Y_1}$ and $\boldsymbol{Y_2}$ responses and have a favorable effect on catalytic

Table 5 Original components of the design matrix and experimental and predict responses obtained for each composition

Exp. no	Point type*	Coded component	Iodine value (IV)			Linoleic acid conversion (%)		
			Experimental	SE	Predicted	Experimental	SE	Predicted
1	1	*A*	94.00	0.0163	93.91	35.00	0.0141	35.16
2	2	*B*	83.00	0.001	83.00	57.24	0.0142	57.08
3	2	*C*	86.00	0.0342	86.19	51.62	0.0424	51.14
4	− 1	*D*	84.00	0.0812	84.45	55.03	0.0432	54.54
5	1	*E*	94.00	0.0162	93.91	35.00	0.0141	35.16
6	2	*F*	89.00	0.0180	89.10	45.80	0.0283	45.48
7	2	*G*	87.00	0.0161	86.91	49.00	0.0001	49.00
8	0	*H*	78.00	0.0542	78.30	68.90	0.1272	67.46
9	− 1	*I*	80.00	0.1209	79.33	63.10	0.1705	65.03
10	− 1	*J*	79.00	0.0523	79.29	65.30	0.0706	64.50
11	− 1	*K*	82.00	0.0704	81.61	59.00	0.1280	60.45

*1 represents vertex, 2 double blends, 0 center point and -1 represents axial point type

Table 6 Coefficients of each model fitted and their level of significance determined by *P-value*

Component	Iodine value (IV)		Linoleic acid conversion (%)	
	Coefficient(β)	*P*-value	Coefficient (β)	*P*-value
X_1	93.91	< 0.0001***	35.16	0.0002***
X_2	86.19	< 0.0001***	51.14	0.0002***
X_3	89.10	< 0.0001***	45.48	0.0002***
X_1X_2	− 28.18	0.0003***	55.73	0.0014**
X_1X_3	− 18.36	0.0015**	34.73	0.0078**
X_2X_3	− 33.43	0.0002***	64.75	0.0009***
$X_1X_2X_3$	− 68.63	0.0138**	169.78	0.025*

Level of statistical significance: *$P < 0.05$, **$P < 0.02$, ***$P < 0.001$

Table 7 The R^2, *adjusted* R^2, and probability values for the final reduced models (component proportion)

Response	ANOVA			
	F-value	R^2	Adjusted R^2	*P*-value
Iodine value (IV)	195.2	0.9966	0.9915	0.0001
Linoleic acid conversion (%)	92.3	0.9928	0.9821	0.0003

activity. Table 7 summarizes the other results of ANOVA for both models. A smaller P-value and a larger *F*-value indicate more significance of the regression coefficient. Both models exhibited *P*-values less than 0.05, meaning they are significant enough. Besides, the $\boldsymbol{Y_1}$ and $\boldsymbol{Y_2}$ models have *F*-values of 195.25 and 92.33, further indicating the significance level of the models. Another important regression analysis is the determination coefficient ($\boldsymbol{R^2}$) which is a suitable tool for evaluating the fitting quality of a regression model. From Table 7, the determination coefficients of $\boldsymbol{Y_1}$ and $\boldsymbol{Y_2}$ models were found to be 0.9966 and 0.9928, respectively, meaning that the regression models can explain 99% of the variability for soybean oil hydrogenation. Moreover, the values of adjusted $\boldsymbol{R^2}$ are very close to the values of the corresponded $\boldsymbol{R^2}$, this is another evidence for the goodness of fitting of the models. Normal probability and predicted versus actual are two diagnostic plots for the evaluation of regression models. These plots are illustrated in Fig. S4. As can be seen from the normal probability plots, indicated in Fig. S4a, c, all the points of normal probability plots are dispersed in the range of − 8 to + 4 and − 2 to + 5 for ***IV*** and linoleic acid conversion models. Figs. S4b and S4d demonstrate a correlation between predicted and experimental values for both models. Obviously, the data points are well scattered around the reference line, confirming the assumption of constant variance.

For $\boldsymbol{Y_1}$ and $\boldsymbol{Y_2}$ models, the coefficient of variations (CV) are 0.601 and 2.85, respectively. CV generally expresses the ratio of the standard deviation to the mean. Thus, the predicted values of linoleic acid conversion have less variation relative to its means compared with the predicted values of ***IV***. Adequate precision measures the signal-to-noise ratio, and means the adequacy of the model used to navigate

the design space. The Adequate precision values above 4 is acceptable. Herein, the adequate precisions were found to be 38.28 and 26.71 for Y_1 and Y_2, respectively, both of them are greater than 4. Therefore, the suggested models can be applied to navigate the design space.

The contour and 3D surface plots obtained from Design Expert software are depicted in Fig. 5. These plots are used to represent the combination effects of metals (Ni, Cu, and Mg) on the catalytic activity. Fig. 5a, b displays response surface and contour plots of ***IV*** as a function of catalyst composition. As can be seen, the combination of Ni with either Cu or Mg leads to remarkably decreasing ***IV***, which means that catalytic activity increases with the addition of Cu and Mg to Ni. Fig. 5c, d depicts the effect of catalyst composition on linoleic acid conversion. It is clear that the response is maximized where Ni is combined with Cu and Mg by the mass fraction ratio of Ni:Cu:Mg of 3.5:1.3:1. The Ni promoted with Cu and Mg exhibited improved catalytic activity and slower catalyst deactivation. The formation of nickel-metal alloy crystallites is less sensitive to dissolution-re-precipitation during the hydrogenation reaction [27]. Furthermore, the loss of catalytic activity upon hydrogenation process can be related to poisoning the oil (sulfur and phosphorous compounds or heavy metals traces), the presence of some natural complex molecules in oil, leaching metals catalyst from the support, formation of coke and carbon monoxide and type of support [28].

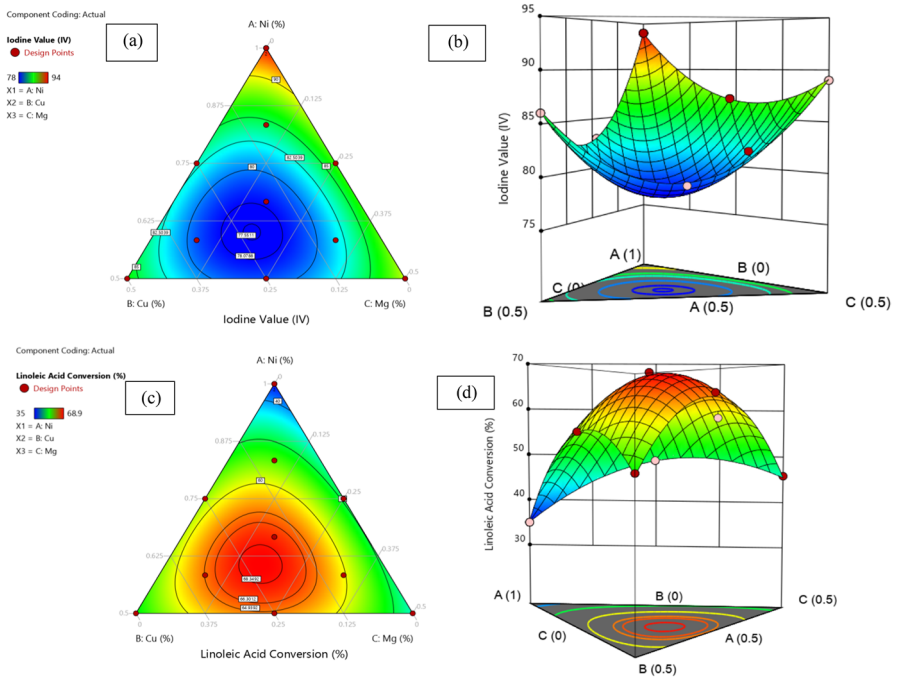

Fig. 5 **a**, **c** Contour, and **b**, **d** 3D surface plots for iodine value and linoleic acid conversion, respectively (under 120 min hydrogenation process in 3 bar H_2 pressure, 180 °C and 900 mL soybean oil)

It is vital to obtain the optimum composition of (Ni–Cu–Mg)/calcined Kieselguhr catalyst for maximizing hydrogenation process. The best composition was found to be 0.6038 Ni, 0.2235 Cu, and 0.1727 Mg by which 77.58 IV and 68.97% linoleic acid conversion are predicted. By applying the best catalyst composition under the same conditions, the experimental results of ***IV*** and linoleic acid conversion were obtained to be 78 ± 0.63 and 70.8 ± 0.43%, respectively. These results are close to those predicted, so the optimum sample can be applied to achieve the best responses. Chemical analysis of the calcined optimum catalyst (Table 2) confirms the presence of activated metal oxides (NiO, CuO and MgO) and the change in sodium value in the composition is negligible.

Fig. 6 demonstrate the results of catalytic hydrogenation of soybean oil by measurement of the fatty acids as a function of time. By the use of (Ni–Cu–Mg)/calcined Kieselguhr catalyst at the optimum condition, linolenic and linoleic acids were converted into oleic and stearic acids. At the end of hydrogenation, the content of linoleic acids reached 5.13%. This small quantity of linoleic acids prevents oil oxidation with air and improves the oil quality. Also, the final content of linolenic acid was 0.29% which is acceptable for edible oil and positively affects human health. The values of oleic and stearic acid were obtained to be 33.48 and 20.65%, respectively, and their changes in the hydrogenation process were 8.26 and 16.64%, respectively. In this condition, the maximum value of trans isomers reached 21.12%, and other undesirables produced from the monoene are

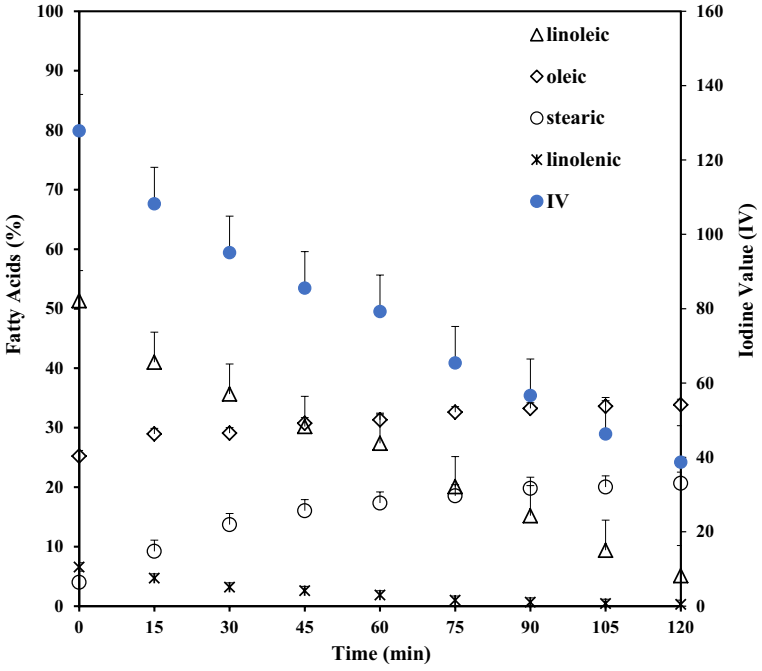

Fig. 6 The content of fatty acids in soybean oil and iodine value during 120 min hydrogenation process in 3 bar H_2 pressure, 180 °C and 900 mL soybean oil

negligible. ***IV*** decreases from 127.84 to 38.75, indicating the progress of hydrogenation reaction and reduction of unsaturated fatty acids.

The rate constant and selectivity for all prepared catalysts were obtained and tabulated in Table 8. It can be seen that $\boldsymbol{k_3 > k_2 > k_1}$, implying that hydrogenation of linolenic and linoleic is faster than that of oleic. The high selectivity in hydrogenation process signifies that the double bond in the carbon chain of linoleic acid is hydrogenated before that of the oleic fatty acid. Higher selectivity means a more desirable oil product. Therein, the optimum catalyst showed the best selectivity among all catalysts.

To clarify the role of Kieselguhr in the catalyst activity, the Ni catalyst and optimum catalyst composition without support were tested. In the same operating conditions, the unsupported catalyst is less active and has lower selectivity in comparing the catalyst supported with Kieselguhr particles.

The effects of catalyst recycling are investigated with the best catalytic composition at operating conditions of 3 bar of hydrogen and 180 °C. Repeated tests of 2 h are conducted to evaluate the efficiency of the catalyst after four cycles. The linoleic acid conversion, IV, and selectivity were analyzed and calculated over four cyclic tests. The results for linoleic acid conversion percentage show a linear trend as a function of the cycle number (Fig. 7). Also observed, the variation of iodine value (*IV*) is limited to 3.1–4.73%. Also. the $\boldsymbol{S}_{\mathrm{Ln}}$ and $\boldsymbol{S}_{\mathrm{Le}}$ selectivity have a decrease of 8.3 and 14.7% over four repeated tests, respectively. By adding fresh catalyst as make-up could solve the catalyst deactivation.

Table 8 The rate constant and the selectivity by the reduced catalysts

Catalyst	k_1 (min^{-1})	$SE \times 10^{-3}$	Rate constants			$SE \times 10^{-3}$	Selectivity	
			k_2 (min^{-1})	$SE \times 10^{-3}$	k_3 (min^{-1})		S_{Ln}	S_{Le}
A	0.0055	0.0629	0.007	0.2872	0.0061	0.1658	0.7858	1.1475
B	0.014	0.7465	0.0076	0.1040	0.007	0.1908	1.8421	1.0857
C	0.0132	0.2496	0.0092	0.1041	0.008	0.1652	1.4349	1.15
D	0.0137	0.1493	0.007	0.1652	0.0066	0.1548	1.9571	1.061
E	0.0054	0.0617	0.0071	0.2887	0.0061	0.1709	0.7605	1.1639
F	0.0104	0.1322	0.0058	0.1931	0.006	0.1109	1.7931	0.9667
G	0.0121	0.2393	0.0068	0.2136	0.0065	0.1250	1.7794	1.0462
H	0.0193	0.2561	0.012	0.2901	0.0089	0.2529	1.6084	1.3483
I	0.0149	0.2658	0.0079	0.3109	0.0072	0.1750	1.8860	1.097
J	0.0192	0.2345	0.0097	0.2097	0.008	0.2529	1.9794	1.2125
K	0.0162	0.2174	0.099	0.2720	0.0078	0.1493	1.8	1.1535
Optimum	0.0258	0.2175	0.0213	0.175	0.0096	0.1040	1.2112	2.2188

SE Standard Error

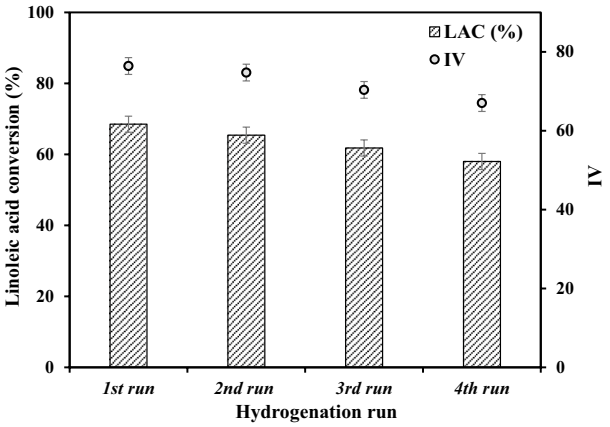

Fig. 7 Linoleic acid conversion (LAC) and iodine value (IV) at 2 h over four repeated tests

Conclusion

The use of experimental design made it possible to find the best quantity of Cu and Mg as promoters of Ni supported on mineral Kieselguhr particles for maximizing the hydrogenation of soybean oil. ***IV*** and linolenic acid conversion were considered as dependent variables. FESEM images revealed that the catalyst particles were uniformly covered the support surface, which is necessary for suitable catalytic activity. The catalytic activity of Ni catalyst was boosted with the addition of Cu and Mg as promoters at the optimum mass fraction of 0.6038 Ni, 0.2235 Cu, and 0.1727 Mg. The optimum catalyst exhibited 78 0.63 and 70.8 0.43 efficiency of IV and linoleic acid conversion. Also, the selectivity of $\boldsymbol{S}_{\mathrm{Ln}} = 1.212$ and $\boldsymbol{S}_{\mathrm{Le}} = 2.218$ was obtained by the best catalyst. The present study claims that Ni promoted by Cu and Mg can be preferred for the soybean oil hydrogenation process.

Supplementary Information The online version contains supplementary material available at https://doi.org/10.1007/s11144-023-02365-4.

Acknowledgements The authors gratefully acknowledge Razi University for the great support to carry out this investigation.

Author contributions All authors contributed to the study conception and design. Material preparation, data collection and analysis were performed by YS, and SS. The first draft of the manuscript was written by SS and all authors commented on previous versions of the manuscript. All authors read and approved the final manuscript.

Funding No funding was received to assist with the preparation of this manuscript.

Data availability All data are provided in the manuscript.

Code availability Not applicable.

Declarations

Conflict of interest The authors declare that they have no conflict of interest.

Ethical approval Not applicable.

Consent to participate All authors made substantial contributions to the conception design, data interpretation, and all steps involved in this work.

Consent for publication All authors have approved the version to be published.

References

1. Cepeda EA, Iriarte-Velasco U, Calvo B, Sierra I (2016) J Am Oil Chem Soc 93:731–741
2. Stanković M, Čupić Z, Gabrovska M, Banković P, Nikolova D, Jovanović D (2015) Reac Kinet Mech Cat 115:105–127
3. Draguez de Hault E, Demoulin A (1984) J Am Oil Chem Soc 61:195–200
4. Gabrovska M, Krstić J, Edreva-Kardjieva R, Stanković M, Jovanović D (2006) Appl Catal A 299:73–83
5. Konkol M, Bicki R, Kondracka M, Antoniak-Jurak K, Wiercioch P, Próchniak W (2016) Reac Kinet Mech Cat 119:595–613
6. Navalikhina MD, Krylov OV (2001) Kinet Catal 42:264–274
7. Zhang L, Xin Z, Liu Z, Wei G, Li Z, Ou Y (2020) Renew Energy 147:695–704
8. Veldsink JW, Bouma MJ, Schöön NH, Beenackers AA (1997) Catal Rev 39:253–318
9. Ferreras JF, Pesquera C, Gonzalez F, Benito I, Blanco C, Renedo J (1994) React Kinet Catal Lett 53:1–6
10. Toshtay K, Auezov AB (2020) Catal Ind 12:7–15
11. Phumpradit S, Reubroycharoen P, Kuchonthara P, Ngamcharussrivichai C, Hinchiranan N (2010) Catalysts 10:993
12. Tacke T, Wieland S, Panster P, Joseph M, DeSimone JM, Tumas W (2004) Green chemistry using liquid and supercritical carbon dioxide. Oxford University Press, Oxford
13. Stanković M, Krstić J, Gabrovska M, Radonjić V, Nikolova D, Lončarević D, Jovanović D (2017) Supported nickel-based catalysts for partial hydrogenation of edible oils. In: Ravanchi MT (ed) New advances in hydrogenation processes-fundamentals and applications. Intech Open, London
14. Cepeda EA, Calvo B, Sierra I, Iriarte-Velasco U (2016) Korean J Chem Eng 33:80–89
15. Vlasova EN, Deliy IV, Nuzhdin AL, Aleksandrov PV, Gerasimov EY, Aleshina GI, Bukhtiyarova GA (2014) Kinet catal 55:481–491
16. Andrade LC, Muchave GJ, Maciel ST, da Silva IP, da Silva GF, Almeida JM, Aranda DA (2022) Int J Chem Eng 40:2004
17. Ojeda M, Osterman N, Dražić G, Fele Žilnik L, Meden A, Kwapinski W, Novak Tušar N (2018) Top Catal 61:1757–1768
18. Song CJ, Park TJ, Moon SH (1992) Korean J Chem Eng 9:159–163
19. Toshtay K, Auyezov AB, Geantet C (2017) Chem Bull Kaz Nat Un 86:4–13
20. Trasarti AF, Segobia DJ, Apesteguía CR, Santoro F, Zaccheria F, Ravasio N (2012) J Am Oil Chem Soc 89:2245–2252
21. Cheng HN, Rau MW, Dowd MK, Easson MW, Condon BD (2014) J Am Oil Chem Soc 91:1461–1469
22. Firestone D (1994) J AOAC Int 77:674–676
23. Schmidt HJ (1968) J Am Oil Chem Soc 45:520–522
24. Gozálvez JM, García-Díaz JC (2006) J Chem Educ 83:647–650
25. Dalanta F, Kusworo TD, Aryanti N, Othman NH (2021) J Environ Chem Eng 9:106517
26. Condon JB (2019) Surface area and porosity determinations by physisorption: measurement. Classical theories and quantum theory. Elsevier, Amsterdam
27. Sotelo-Boyás R, Trejo-Zárraga F, Hernández-Loyo FDJ, Karame I (2012) Hydrogenation 338:338

28. Wang Y, Yang X, Chen Y, Nie S, Xie M (2017) Reac Kinet Mech Cat 122:915–930

Publisher's Note Springer Nature remains neutral with regard to jurisdictional claims in published maps and institutional affiliations.

Springer Nature or its licensor (e.g. a society or other partner) holds exclusive rights to this article under a publishing agreement with the author(s) or other rightsholder(s); author self-archiving of the accepted manuscript version of this article is solely governed by the terms of such publishing agreement and applicable law.